Aerosol and Air Quality Research, 16: 2428–2437, 2016

ISSN: 1680-8584 print / 2071-1409 online
doi: 10.4209/aaqr.2015.07.0466

Assessing the Protection Provided by Facepiece Filtering Respirator: New Model Involving Spherical Porous Layer with Annular Peripheral Opening

Ilnar T. Mukhametzanov[1], Sergey A. Grinshpun[2*], Shamil K. Zaripov[1*], Artur K. Gilfanov[1]

[1] *Kazan Federal University, Kazan 420008, Russia*
[2] *Center for Health-Related Aerosol Studies, University of Cincinnati, Ohio 45267-0056, USA*

ABSTRACT

The penetration of aerosol particles inside a facepiece filtering respirator (FFR) was investigated using a novel model, which involved a spherical porous layer representing a filter and an annular peripheral opening representing a faceseal leakage. The model utilized a two-dimensional laminar incompressible flow in a free space and porous zones that are numerically solved by a computational fluid dynamic code FLUENT. Following the model validation, the efficiency of an FFR with an annular faceseal leakage opening was investigated as a function of the inhalation flow rate, particle size, and the ratio of the leak-to-filter areas. The filter material permeability was determined for a conventional N95 filter medium. It was found – for two inhalation flow rates (Q_i = 30 and 85 L min^{-1}) and three particle diameters (d_p = 50 nm, 100 nm and 1 μm) – that once the faceseal leakage area exceeded 0.1% of the total surface of an N95 facepiece, the respirator was unable to offer the 95% protection – the minimum level that should be provided by its filter. It was demonstrated that under certain leakage condition (partially determined by the inhalation flow rate), the respirator protection level becomes independent on the particle size; furthermore, it is not anymore affected by the efficiency of its filter, and is only influenced by the size of the faceseal leakage.

Keywords: Respiratory protection; Penetration; Filter; Faceseal leakage; CFD.

INTRODUCTION

Facepiece filtering respirators (FFRs) are widely used for protecting the human respiratory system from various aerosol hazards. Inhalation of ultrafine/nano-scale (< 0.1 μm) and fine (< 2.5 μm) particles is of significant concern because these particles can penetrate to the lower sections of the respiratory tract and cause health problems. The protection offered by an FFR is often determined by measuring the efficiency of a respirator filter. E.g., the National Institute for Occupational Safety and Health (NIOSH) grants a respiratory protection device an N95/R95/P95 certification if the collection efficiency of its filter is at least 95%. However, the respirator performance also depends on the fit, which involves the respirator peripheral area because – beyond the filter media – the particles may readily penetrate through the faceseal leakage (Fig. 1(a)).

Experimental studies, e.g., Chen and Willeke (1992) and Grinshpun *et al.* (2009), have demonstrated that even small faceseal leakage can considerably decrease the protection level offered by a facemask. The particle flux through a leak depends on factors such as the breathing flow rate, particle size, leak size, and filter air permeability.

The manikin-based performance evaluation of faceseal filtering respirators and masks with artificial leaks (both peripheral and in-filter ones) was conducted by several investigators, including Hinds and Kraske (1987), Chen and Willeke (1992), Lee *et al.* (2005), Rengasamy and Eimer (2011) and Rengasamy and Eimer (2012). The effect of the faceseal leakage on the particle penetration inside a respiratory protection device was discussed by Grinshpun *et al.* (2009), Cho *et al.* (2010), He *et al.* (2014) and others. Modeling of the protection offered by a non-perfectly fit FFR is important for predicting the actual aerosol exposure for a wearer and optimizing the design of respirators. A 3D computational fluid dynamic (CFD) model developed by Lei *et al.* (2013) for a human head geometry demonstrated that faceseal leaks are primarily formed in the nose area as well as under the chin; however, the contributions of the particle penetrations through the filter and the faceseal leakage remain insufficiently characterized. A parametric study utilizing a user-friendly mathematical model would be useful for predicting the protection of respirator as a function the breathing regime, particles size, leak size, filter material permeability, and other variables.

* Corresponding author.
Tel.: 1-513-558-0504; Fax: 1-513-558-2263
E-mail address: sergey.grinshpun@uc.edu;
shamil.zaripov@kpfu.ru

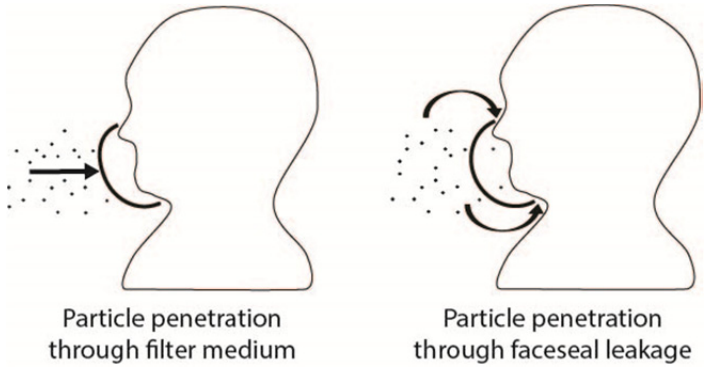

Fig. 1(a). Two particle penetration pathways (adopted from Grinshpun *et al.* (2009)).

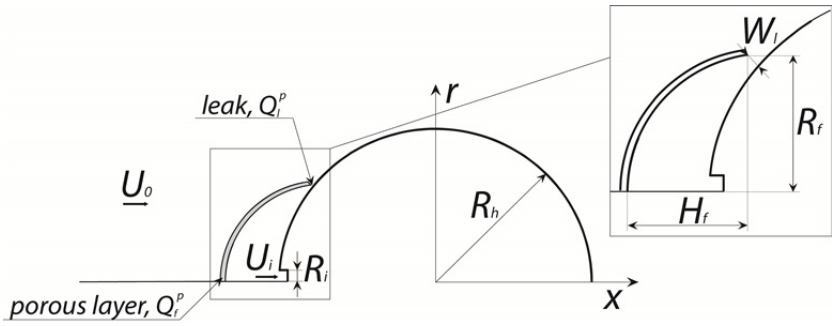

Fig. 1(b). Schematics used for modeling.

Our recent investigation of the aspiration efficiency of an idealized spherical sampler in a slow moving air (Zaripov *et al.*, 2014) has shown that the aerosol fraction inhaled by a manikin headform can be successfully described using the well-developed concept of aerosol aspiration into a blunt sampler. In the present effort, we utilized the spherical sampler model to describe the air flow through an FFR during inhalation. The shape of most of commercial respirator facepieces is close to spherical. Consequently, a spherical segment was selected as a reasonable approximation. This fits the two-dimensional fluid flow model. The respirator filter was represented by a porous spherical layer that was loosely attached to the head creating a faceseal leakage approximated by a narrow annular slot. The latter approximation is different from those previously investigated (Chen and Willeke, 1992; Lei *et al.*, 2013). Due to the facial muscle motion and the head movements, the faceseal leakage size and shape constantly change, suggesting that any approximation chosen is not fully representative. The air flow was defined as an axisymmetric stationary laminar flow in the combined free-space and porous domains. The permeability of the filter material used in the newly-developed model was determined by fitting the available experimental data. Using this model, the respiratory protection provided by an FFR was numerically examined as a function of the breathing flow, particle size, and the ratio of the leak-to-filter areas.

THEORETICAL FOUNDATION

The human head was approximated by a sphere (radius R_h) with a circular orifice for breathing (radius R_i) as shown in the symmetry plane of cylindrical coordinate system (x, r) in Fig. 1(b). The steady flow model that has been used in the past to estimate the filtration characteristics of the respirators with leaks (Liu *et al.*, 1993), can be applied to both the leak and the respirator filter (in this case, no effects associated with cyclic breathing is considered). The air movement in the breathing zone (governing the aerosol transport from the ambient environment into a respirator cavity) was approximated by an axisymmetric stationary flow passing through

(i) a porous layer simulating the filter and defined by height H_f of the spherical segment and radius R_f of its base and.

(ii) an annular peripheral opening simulating the faceseal leak defined by width W_l.

The air velocity, which is constant (U_0) far from the sphere, changes in its vicinity as the air moves around the spherical body (head) and, at the same time, is being aspirated due to inhalation. In absence of the porous layer, the above represents a well-established fluid mechanics problem describing an aerosol aspiration from moving air into a spherical sampler (Dunnett and Vincent, 2000; Galeev and Zaripov, 2003).

The air flow was assumed to be two-dimensional, laminar, incompressible and steady. The single-domain approach (Basu and Khalili, 1999; Bhattacharyya *et al.*, 2006) was applied to simulate the fluid in the environment outside and inside of the porous layer. To numerically solve the fluid flow equations, we chose to use the ANSYS/FLUENT code. The axisymmetric laminar viscous flow in the free space and homogeneous porous medium are described by

the following equations (ANSYS, 2009):

$$\frac{\partial u_r}{\partial r}+\frac{u_r}{r}+\frac{\partial u_x}{\partial x}=0 \tag{1}$$

$$\begin{aligned}&\frac{1}{r}\frac{\partial\left(r\rho u_x u_x\right)}{\partial x}+\frac{1}{r}\frac{\partial\left(r\rho u_r u_x\right)}{\partial r}\\&=-\frac{\partial P}{\partial x}+\frac{1}{r}\frac{\partial}{\partial x}\left[r\mu\left(2\frac{\partial u_x}{\partial x}-\frac{2}{3}\left(\nabla\cdot\vec{u}\right)\right)\right]\\&+\frac{1}{r}\frac{\partial}{\partial r}\left[r\mu\left(\frac{\partial u_x}{\partial r}+\frac{\partial u_r}{\partial x}\right)\right]-m\frac{\mu}{k}u_x\end{aligned} \tag{2}$$

$$\begin{aligned}&\frac{1}{r}\frac{\partial\left(r\rho u_x u_r\right)}{\partial x}+\frac{1}{r}\frac{\partial\left(r\rho u_r u_r\right)}{\partial r}\\&=-\frac{\partial P}{\partial r}+\frac{1}{r}\frac{\partial}{\partial r}\left[r\mu\left(2\frac{\partial u_r}{\partial r}-\frac{2}{3}\left(\nabla\cdot\vec{u}\right)\right)\right]\\&+\frac{1}{r}\frac{\partial}{\partial x}\left[r\mu\left(\frac{\partial u_x}{\partial r}+\frac{\partial u_r}{\partial x}\right)\right]\\&-2\mu\frac{u_r}{r^2}+\frac{2}{3}\frac{\mu}{r}\left(\nabla\cdot\vec{u}\right)-m\frac{\mu}{k}u_r\end{aligned} \tag{3}$$

Here u_x, u_r are the gas velocity components in a cylindrical coordinate system (x, r), μ is the air viscosity, ρ is the air density, P is the pressure, and k is the permeability of a porous medium. In the free zone (m = 0), Eqs. (1)–(3) turn into the Navier-Stokes equations. Within the porous region (m = 1), Eqs. (1)–(3) turn into the modified Navier-Stokes equations with an additional Darcy term that takes into account a viscous resistance term 1/k. The inertial resistance term was neglected due to small Reynolds number for the filtration flow velocity within the porous medium.

The above governing equations are subject to boundary conditions. The two-dimensional computational domain is considered as a region between the outer circular boundary and the sphere surface. On the left half of the outer circular boundary of the calculation domain, the fluid velocity equals to U_0 (defined as "inlet conditions" in FLUENT), and on the right half of the outer circular boundary the pressure equals to the atmospheric pressure (defined as "outlet conditions" in FLUENT). On the inner spherical surface (r = R_h), u_x = 0, u_r = 0. The air velocity at the cross-section of the circular suction orifice is defined as the inhalation velocity U_i. The symmetry boundary conditions are applied along the x-axis.

The respirator protection factor, PF, is defined as a ratio of the ambient aerosol particle concentration, C_0, to the particle concentration inside the respirator, C_i. The protection factor and leakage flow can be determined using the assumption of particle conservation inside and outside the respirator (Liu *et al.*, 1993). The theoretical and experimental studies presented by Liu *et al.* (1993) for circular leaks have shown that the protection factor of the respirator was strongly influenced by the filter efficiency, the leak size and the flow rate through the respirator. The lower particle size limit used in this effort was 10 nm. For air velocities typical for human breathing, the diffusional deposition of particles with d_p > 10 nm can be neglected (Gradon and Yu, 1989). The upper limit of the particle size considered in this study was 1000 nm, which allows neglecting the particle inertia. The fluid flow model is assumed to be laminar as the Reynolds number was estimated to be approximately 1200 (see below); thus, the turbulent dispersion of the particles was neglected.

The particle balance equation for the aerosol flow into a respirator cavity can be presented as

$$C_0 Q_f \eta_f + C_0 Q_l \eta_l = C_i Q_i \tag{4}$$

where Q_f and Q_l are respective air flow rates through the filter and the faceseal leakage, $Q_i = U_i \pi R_i^2 = Q_f + Q_l$ is the inhalation air flow rate, η_f and η_l are the particle penetrations through the filter and leak, respectively. Consequently (Myers *et al.*, 1986),

$$PF = \frac{C_0}{C_i} = \frac{Q_i}{Q_f \eta_f + Q_l \eta_l} \tag{5}$$

The Total Inward Leakage (TIL), a commonly used quantitative characteristic of the protection provided by a respirator, is an inverse value of PF:

$$TIL = \frac{Q_f \eta_f + Q_l \eta_l}{Q_i} \tag{6}$$

To utilize Eq. (6), one needs to know the respective air flow rates through the filter and the faceseal leakage, Q_f and Q_l, which can be found from the numerical solution of Eqs. (1)–(3) for the various values of Q_i.

The particle motion inside the filter is affected by multiple mechanisms, including particle inertia, gravity, interception, diffusion, and electrostatic interaction. The relative contributions of these mechanisms are largely determined by the particle size. The particle penetration through a respirator filter with a thickness L and packing density α, which consists of fibers with a diameter d_{fiber}, can be obtained using the classic theory of depth filtration (Pich, 1966):

$$\eta_f = \exp\left(-\frac{4\alpha E_{fiber} L}{\pi d_{fiber}(1-\alpha)}\right) \tag{7}$$

where E_{fiber} is the collection efficiency of a single fiber, which can be expressed as

$$E_{fiber} = 1 - (1 - E_r)(1 - E_d)(1 - E_q) \tag{8}$$

where E_r, E_d, E_q are the collection efficiencies of a single fiber due to interception, diffusion and electrostatic deposition respectively. Eq. (8) assumes that the particles are small enough to make the inertial and gravitational components negligible.

The E_d-value can be calculated (Payet *et al.*, 1992; Gougeon *et al.*, 1996) as follows:

$$E_d = 1.6\beta \mathrm{Pe}^{-2/3} c_d c_d^*$$
$$\beta = \left(\frac{1-\alpha}{\mathrm{Ku}}\right)^{1/3},$$
$$c_d = 1 + 0.388 \mathrm{Kn}_{fiber} \beta \mathrm{Pe}^{1/3}, \quad (9)$$
$$c_d^* = \left(1 + 1.6\beta \mathrm{Pe}^{-2/3} c_d\right)^{-1}$$

where Pe = $U_f d_{fiber}/D$ is the Peclet number, U_f is the air filtration velocity through the porous filter medium, D = $k_b T C_c/3\pi\mu d_p$ is the diffusion coefficient (Hinds, 1998), d_p is the particle diameter $k_b = 1.381 \times 10^{-23}$ J K^{-1} is the Boltzmann constant, T = 298 K is the air temperature, $\mathrm{Kn}_{fiber} = 2\lambda/d_{fiber}$, λ is the gas mean free path, and Ku is the Kuwabara hydrodynamic factor calculated as

$$\mathrm{Ku} = -0.5\ln\alpha - 0.75 + \alpha - 0.25\alpha^2 \quad (10)$$

According to Hinds (1998), the Cunningham slip correction factor in the diffusion coefficient is determined as

$$C_c = 1 + \mathrm{Kn}[1.142 + 0.558 \exp(-0.999/\mathrm{Kn})] \quad (11)$$

where $\mathrm{Kn} = 2\lambda/d_p$ is the particle Knudsen number.

The E_r value can be calculated (Payet *et al*., 1992; Gougeon *et al.*, 1996) as follows:

$$E_r = 0.6\left(\frac{1-\alpha}{\mathrm{Ku}}\right)\frac{N_r^2}{(1+N_r)} c_r, \quad c_r = 1 + \frac{1.9996\mathrm{Kn}_{fiber}}{N_r} \quad (12)$$

where $N_r = d_p/d_{fiber}$ is the interception parameter.

The commercially available facepieces are usually made of charged fibers (electret filter media) so that the aerosol particles passing through this media are polarized by the electric field (with dipole charges are induced on them). The coulombic forces were not considered since we assumed that the particles are not charged. The particle penetration determined under this assumption is believed to represent the worst case scenario, i.e., the most conservative case. For the same reason, the National Institute for Occupational Safety and Health (NIOSH) uses charge-equilibrated ("neutralized") particles for the respirator certification program. A simple estimation shows that the *TIL* decreases when the particles are charged, primarily due to and enhanced deposition of charged particles on fibers (governed by the coulombic forces, which depend on the particle charge). Since the particles may carry different charges, the charge was excluded as a less-than-desirable uncertainty and the most conservative case was pursued. As the filter fibers are charged, the polarization mechanism is still in effect (regardless of whether the particles are charged or neutral). The collection efficiency E_q accounting for the electrostatic deposition due to the polarization forces can be determined (Kanaoka *et al*., 1987) as follows:

$$E_q = 0.06 N_{Q0}^{2/5} \quad (13)$$

where

$$N_{Q0} = \frac{C_c q^2 d_p^2 (\varepsilon_{fiber} - 1)}{3\pi^2 \varepsilon_0 \mu d_{fiber}^3 U_f (\varepsilon_{fiber} + 2)} \quad (14)$$

Here q is the charge density of a single fiber, which may be specific to a filter material [e.g., Bałazy *et al.* (2006) determined q = 13 nC m^{-1} for their experimental conditions], ε_{fiber} is the relative permittivity of the fiber, which also varies from one filter material to another [we found that ε_{fiber} = 4 can be adopted for N95 filters (Bałazy *et al*.; 2006)], and ε_0 = $8.85 \cdot 10^{-12}$ F m^{-1} is the vacuum permittivity.

SELECTION OF PARAMETERS AND MODEL VALIDATION

In this study, the human head was approximated by a sphere, and the air flow and particle motion was studied within a circular cross-section of a specific radius (a two-dimensional configuration shown in Fig. 1(b)). To determine this radius, we reviewed an earlier experimental study of Kennedy and Hinds (2002) in which the investigators used a headform having an elliptical cross-section with a height, H_h, of 0.225 m and diameter, D_h, of 0.134 m. The latter produced an area of S = 0.0237 m^2. This is equivalent to a circular area of a radius R_h = 0.087 m, which we rounded to 0.09 m. The selected dimensions are consistent with other reports [e.g., Yang *et al.* (2009) referred to H_h = 0.15–0.16 m and D_h =0.14–0.15 m, and Anthony (2010) listed H_h = 0.216 m and D_h = 0.142 m]. In our model, the inhalation flow was applied to an orifice of a radius R_i = 0.007 m, which represents a mouth breathing through an area of S_i = 0.000154 m^2. This is between the values of S_i = 0.0001386 m^2 used in the digital head model of Anthony and Flynn (2005) and S_i = 0.00016 m^2 used for the mouth area in manikin-based experiments of Kennedy and Hinds (2002). This configuration is analogous to a spherical aerosol sampler that has a radius of R_h = 0.09 m and a point-like opening of R_i = 0.007 m.

The filter porous layer was approximated by a spherical segment with a height of H_f = 0.05 m and a base radius of R_f = 0.057 m (Fig. 1(b)). This produced a filter area of $S_f = \pi(R_h^2 + R_f^2)$ = 0.018 m^2, which is consistent with conventional respirator facepieces such as European FFP2 and American N95 FFRs for which S_f = 0.0158–0.0255 m^2 (Roberge *et al*., 2010). To establish the leaks of various sizes, we varied the location of the spherical segment relative to the sphere by moving the segment along the x-axis (Fig. 1(b)). As a result, we investigated annular peripheral leaks of different widths, W_l, and annular slot areas, S_l.

The inhalation flow rates Q_i were selected to represent different levels of human physical activity, including Q_i = 6–8 L min^{-1} (at rest), 30 and to 40 L min^{-1} (a moderate work load), and 85 L min^{-1} (a heavy work load). The flow rate of 85 L min^{-1} is also used in the NIOSH certification testing (NIOSH, 1996). A mid-level flow rate of 30 L min^{-1} was utilized to fit the filter penetration values, which were experimentally obtained by Rengasamy and Eimer (2012)

to the model for η_f. This allowed us to determine the parameters of porous layer representing an N95 filter. The next step was to validate the entire model by comparing the calculated *TIL* values to the experimental *TIL* data available from the quoted study for two flow rates, 8 and 40 L min^{-1}. Finally, the parametric study of *TIL* was performed utilizing the new model with two most practically relevant flow rates, 30 and 85 L min^{-1}.

The flow rates of Q_i = 8, 30, 40, and 85 L min^{-1} produced the following average inhalation velocities through the above-defined annular circle orifice: U_i = 0.870, 3.25, 4.33, and 9.20 m s^{-1}, respectively. The ambient air velocity, U_0, was assumed to be 0.1 m s^{-1} representing a typical calm indoor air environment (Zhang, 2004). The air flow Reynolds number calculated for a sphere diameter of R_h = 0.09 m and a wind velocity of U_0 = 0.1 m s^{-1} is Re = 1200 that represents the laminar-to-transitional regime; it is certainly below the turbulent level allowing to use a laminar fluid model.

The outer boundary dimensions were established for the calculation domain so that the influence of the spherical body on the fluid flow was negligible: R_b = 20 m.

A conventional N95 filter has three layers. In this study, we approximated it by a single-layer filter with a thickness of L = 0.003 m and a fiber packing density of α = 0.069 (Rengasamy and Eimer, 2012). The theoretical model of particle penetration described by Eqs. (7)–(14) includes the air velocity through the filter, U_f. The value of U_f was calculated as the ratio of Q_f/S_f using the value of Q_f obtained from the numerical solution of the fluid flow equations. The least square method was used to determine the fiber diameter d_{fiber}, which provided the best fit of the theoretical particle penetration $\eta_f(d_p)$ to the experimental curve obtained by Rengasamy and Eimer (2012) at Q_i = 30 L min^{-1}. The derived fiber diameter value, 10.07 μm, was further used in the modeling. The theoretical and experimental curves for the particle penetration $\eta_f(d_p)$ through the filter are presented in Fig. 2.

To find a solution of Eqs. (1)–(3), the aerodynamic drag value in the porous medium needs to be calculated. This is an inverse quantity to its permeability, *k*. If the porous medium is approximated by an array of cylinders (fibers), *k* can be obtained through the Kozeny-Carman equation (Nield and Bejan, 1992):

$$k = \frac{\varepsilon^3 d_{fiber}^2}{180(1-\varepsilon)^2} \tag{15}$$

where $\varepsilon = 1 - \alpha$. For d_{fiber} = 10.07 μm and α = 0.069, Eq. (15) produces $k = 9.55 \times 10^{-11}$ m^2.

For practical purposes, the air permeability, A_p, is used as an alternative to *k* for characterizing the filter properties (Li *et al*., 2006):

$$A_p = \frac{Q}{S_f \Delta P} \tag{16}$$

Here ΔP is the pressure drop. Using the Darcy law for porous filter medium $\Delta P/L = \mu U_f/k$ and Eq. (16), the permeability *k* can be expressed as

$$k = \frac{U_f L \mu}{\Delta P} = A_p L \mu \tag{17}$$

Adopting $A_p = 12.5 \times 10^4$ mL s^{-1} m^{-2} and ΔP = 100 Pa from Li *et al.* (2006) (determined for an N95 fiber medium with L = 0.00387 m), we found $k_{N95} = 8.85 \times 10^{-11}$ m^2. This is very close to the value of $k_{N95} = 8.9 \times 10^{-11}$ m^2 determined by Lei *et al.* (2013) based on the experimental data reported by Li *et al.* (2006). Thus, the permeability value obtained through the alternative calculation as well as the value available from the literature are consistent with $k = 9.55 \times 10^{-11}$ m^2 obtained from Eq. (15) using d_{fiber} = 10.07 μm (see above). Consequently, the filter permeability of $k = 9.55 \times 10^{-11}$ m^2 was further used for calculations.

The system of Eqs. (1)–(3) was solved by the finite volume method using ANSYS/FLUENT. The segregated steady-state solver was used. The second order upwind discretization scheme was applied for the momentum equations. The SIMPLE algorithm was chosen for the pressure-velocity coupling (ANSYS, 2009). The unstructured grid used for

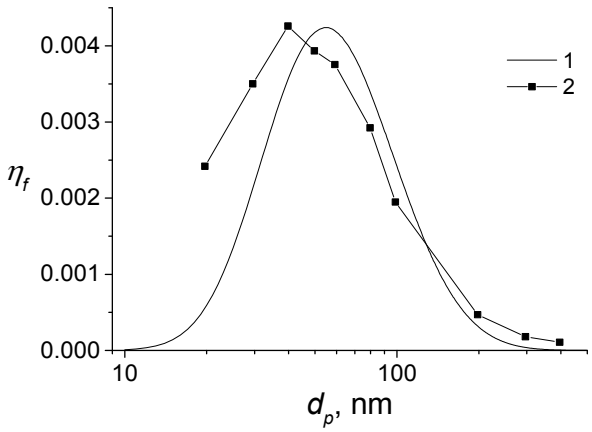

Fig. 2. The particle penetration through the filter, η_f, as a function of the particle size, d_p, at Q_i = 30 L min^{-1}: 1 – calculated from Eqs. (7)–(14) at d_{fiber} = 10.07 μm, 2 – experimental values from Rengasamy and Eimer (2012).

the calculation domain with a denser mesh near the boundary between the free space and the porous layer provides the convergence of the numerical solution with the relative residual of 10^{-10}. Additionally, the grid was constructed in a way that at least ten finite volumes (cells) were accommodated in the cross-section of a peripheral opening. To check the grid independence of the numerical solution, the gas fluxes through the leaks of various sizes were calculated. The values of O_l calculated at Q_i = 30 L min^{-1} for three selected leakage-to-filter area ratios (S_l/S_f) and three grid sizes (course, medium, and fine) that correspond to different numbers of cells are presented in Table 1. The differences between the results obtained for grid sizes 1, 2 and 3 were evaluated, and grid 2 was chosen as a reasonable approximation (accounting for the precision-cost balance).

The unstructured grid and the set of streamlines calculated in the vicinity of the inhalation orifice for W_l = 1 mm, Q_i = 30 L min^{-1}, and $k = 9.55 \times 10^{-11}$ m^2 are respectively shown in Figs. 3(a) and 3(b). The flow rate Q_l through leakage is found by integration of the air velocity in the cross-section of an annular peripheral opening using the corresponding function of the ANSYS/FLUENT code. The value of Q_f can be then calculated as $Q_f = Q_i - Q_l$. No losses during the particle penetration through leak (η_l = 1) was postulated due to the very small depth of the opening. The particle penetration through the filter η_f is calculated from the approximate theoretical model, Eqs. (7)–(9), (12), and (13), for the permeability value obtained with the best fit approach.

To validate the model developed in this effort, we used the experimental data presented by Rengasamy and Eimer (2012) for an N95 FFR with two circular holes in the filter of D_h = 1.8 and 3 mm in diameter. Unlike some previous studies, including Rengasamy and Eimer (2012), our model defines the faceseal leakage of an annular shape, which is believed to be more realistic than a single- or double-hole configuration. For the leak, two widths, W_l = 0.0142 and 0.0395 mm, producing the annular slot areas of S_l = 5.09 и 14.14 mm^2, respectively, were chosen to match the areas used in the Rengasamy and Eimer (2012) study. It is acknowledged that the quoted investigation used a cyclic regime while we applied a constant flow. Given that *TIL* = 0 over half of the time in a cycle (during exhalation), the experimental data, which we used for matching, reflected an equivalent of 1/2 of the *TIL* value predicted by our model. To account for this difference, a correction factor of 2 was introduced in the validation effort. This correction factor produced the following revised values of S_l: 10.18 and 28.28 mm^2. The *TIL* values calculated with the correction factor deployed are shown in Fig. 4 for Q_i = 8 and 40 L min^{-1}. The experimentally obtained *TIL* values reported by Rengasamy and Eimer (2012) for the two flow rates are also shown in this figure. The agreement between the experimental results and the model seems fair. At the lower flow rate, Q_i = 8 L min^{-1}, the calculated *TIL* was not dependent on the particle size for both chosen dimensions of the faceseal leakage (Fig. 4(a)), while at Q_i = 40 L min^{-1} the model predicted the particle size dependent penetration with the most penetrating particle size close to 50 nm. The latter was also observed in the quoted experiments (Fig. 4(b)). It was observed in the experiments of Rengasamy and Eimer (2012) and confirmed by our calculations that the value of *TIL* increases with flow rate decrease and that its dependence on the particle size becomes weak at low flow rates. A constant (not size dependent) *TIL* for a larger leak area suggests that the particles penetrate primarily through the leakage. In the case of a small leak, we obtained *TIL* = constant due to a weak dependence of the penetration efficiency on the particle size. The particle size dependence of

Table 1. Effect of the grid size on the air flux through the leak for various leakage-to-filter area ratios (S_l/S_f) at Q_i = 30 L min^{-1}.

Grid size	Leakage-to-Filter Area Ratio, S_l/S_f					
	8×10^{-5}		8×10^{-4}		2×10^{-2}	
	Number of cells	Q_l, L min^{-1}	Number of cells	Q_l, L min^{-1}	Number of cells	Q_l, L min^{-1}
1	260405	0.01434	103832	1.0374	99809	25.02
2	435148	0.01308	176706	1.0470	173440	23.70
3	613802	0.01284	392765	1.0470	397545	24.06

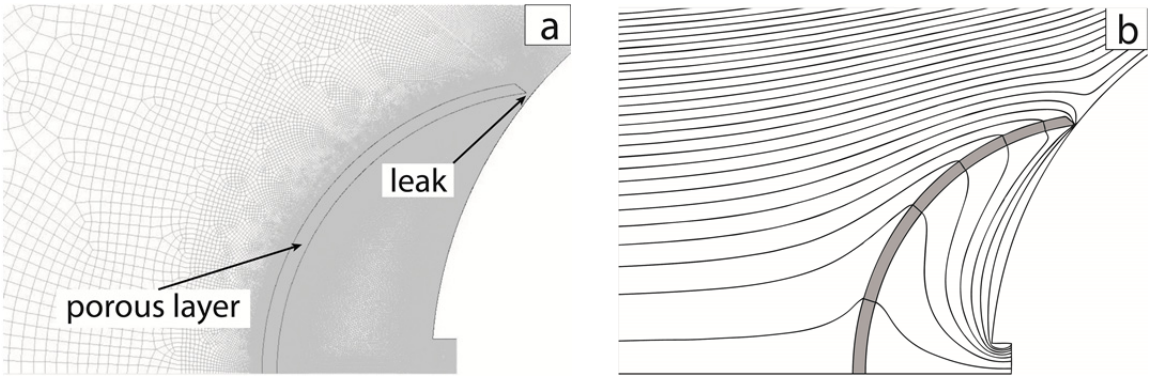

Fig. 3. The unstructured grid near the inhalation orifice (*a*) and the streamlines for the flow through the porous layer (*b*). Calculated for W_l = 1 mm, Q_i = 30 L min^{-1}, and $k = 9.55 \times 10^{-11}$ m^2.

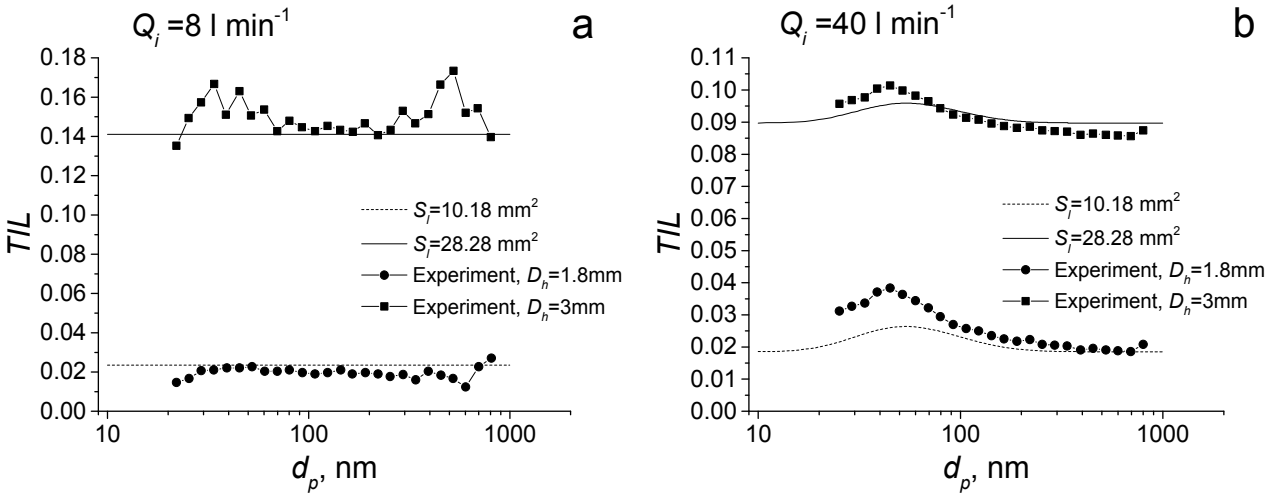

Fig. 4. *TIL* as a function of d_p at Q_i = 8 L min^{-1} (a) and 40 L min^{-1} (b): data from the newly-developed model compared to the experimental data from Rengasamy and Eimer (2012).

TIL with an apparent most penetrating particle size points to a measurable contribution of particles penetrating inside the respirator through the filter material. It is seen that the experimental *TIL* values "fluctuate" although we found no clear reason for this behavior; perhaps, it may be associated with a flow turbulence (Rengasamy and Eimer, 2012).

In summary, the model was validated and found suitable for assessing the performances of a filtering facepiece in presence of a faceseal leakage.

RESULTS AND DISCUSSION

Fig. 5 presents *TIL* as a function of d_p calculated using the newly-developed model at two inhalation flow rates, 30 and 85 L min^{-1}, and different leakage-to-filter area ratios, S_l/S_f : 2×10^{-2}, 4×10^{-3}, 8×10^{-4}, and 8×10^{-5}. The chosen range covers the two values quoted by Rengasamy and Eimer (2012). *TIL* increases with increasing S_l/S_f. At Q_i= 30 L min^{-1} and W_l = 1 mm ($S_l/S_f \approx 2 \times 10^{-2}$), the model predicts *TIL* close to the unity (essentially, no protection), suggesting that the air flow enters the respirator cavity primarily through the faceseal leakage (the air flow and thus the particle flux through the porous filter layer are negligible). It is seen that under these conditions *TIL* is independent on the particle size, which is explainable given that the particles essentially have no inertia. As the relative leak size S_l/S_f decreases to ~10^{-4} to 10^{-3} (depending on the flow rate), *TIL* becomes particle size dependent (see the non-monotonic curves in Fig. 5 at lower S_l/S_f). This serves as an evidence of a significant aerosol particle flux through the filter. The above S_l/S_f range corresponds to a leak width of ~10^{-2} to 10^{-1} mm. The data show the highest penetration occurring for particle sizes between 40 and 70 nm. This is consistent with the conventional filtration theory and the experimental data published by Bałazy *et al.* (2006) for the N95 filters. Increase in the contribution of filter penetration over the faceseal leakage, which was observed with the decrease of the leak area, is more pronounced at higher inhalation flow rates, as seen from the comparison of the data obtained at 30 versus 85 L min^{-1} (Fig. 5). A significant practical outcome of the above is that the filter efficiency has essentially no influence on the protection offered by the respirator once a faceseal leakage area reaches ~0.1% or greater of the respirator area for the N95 FFR considered in this study. For a typical inhalation flow rate, this area can be formed by an annular circular slot with a width of W_l~0.05 mm.

Fig. 6 presents *TIL* as a function of S_l/S_f calculated using the new model at two inhalation flow rates (Q_i = 30 and 85 L min^{-1}) and three particle diameters (d_p = 50 nm, 100 nm and 1 μm). The solid horizontal lines corresponding to *TIL* = 0.05 represent the target value for an N95 respirator filter. The dotted horizontal lines in Figs. 6(a) and 6(b) correspond to the values calculated for a respirator worn with no faceseal leakage at the respective flow rates Q_i = 30 and 85 L min^{-1}. Similar dotted lines are not seen in Fig. 6(c) because for the particles as large as 1 μm the no-leak scenario generates extremely low *TIL* (~10^{-7}), which are beyond the scale of this plot (the case has little practical significance). The model applied to an N95 FFR predicts that *TIL* is an increasing function of S_l/S_f that intersects the 95% filter efficiency threshold at S_l/S_f ~10^{-3} for both flow rates and the three tested particle sizes. It means that the value of S_l/S_f ~10^{-3} can be considered as the limit above which the faceseal leakage does not allow the N95 respirator to offer the 95% protection level that is provided by its filter.

The results suggest that the relative leakage area, introduced in this study (S_l/S_f), is a major factor contributing to the protection provided by a respirator that has no perfect fit, along with the breathing flow rate and the particle penetration through the filter layer.

CONCLUSIONS

The model for predicting the protection provided by a facepiece filtering respirator in presence of an annular faceseal leakage was developed, validated and utilized for different inhalation flow rates, particle sizes, and leakage

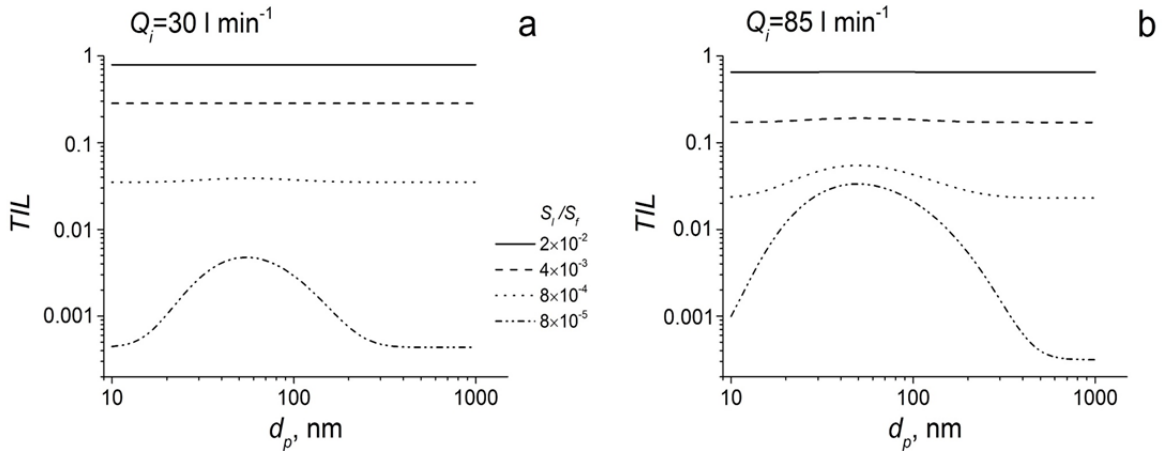

Fig. 5. *TIL* as a function of d_p calculated using the newly-developed model at Q_i = 30 L min^{-1} (a) and 85 L min^{-1} (b).

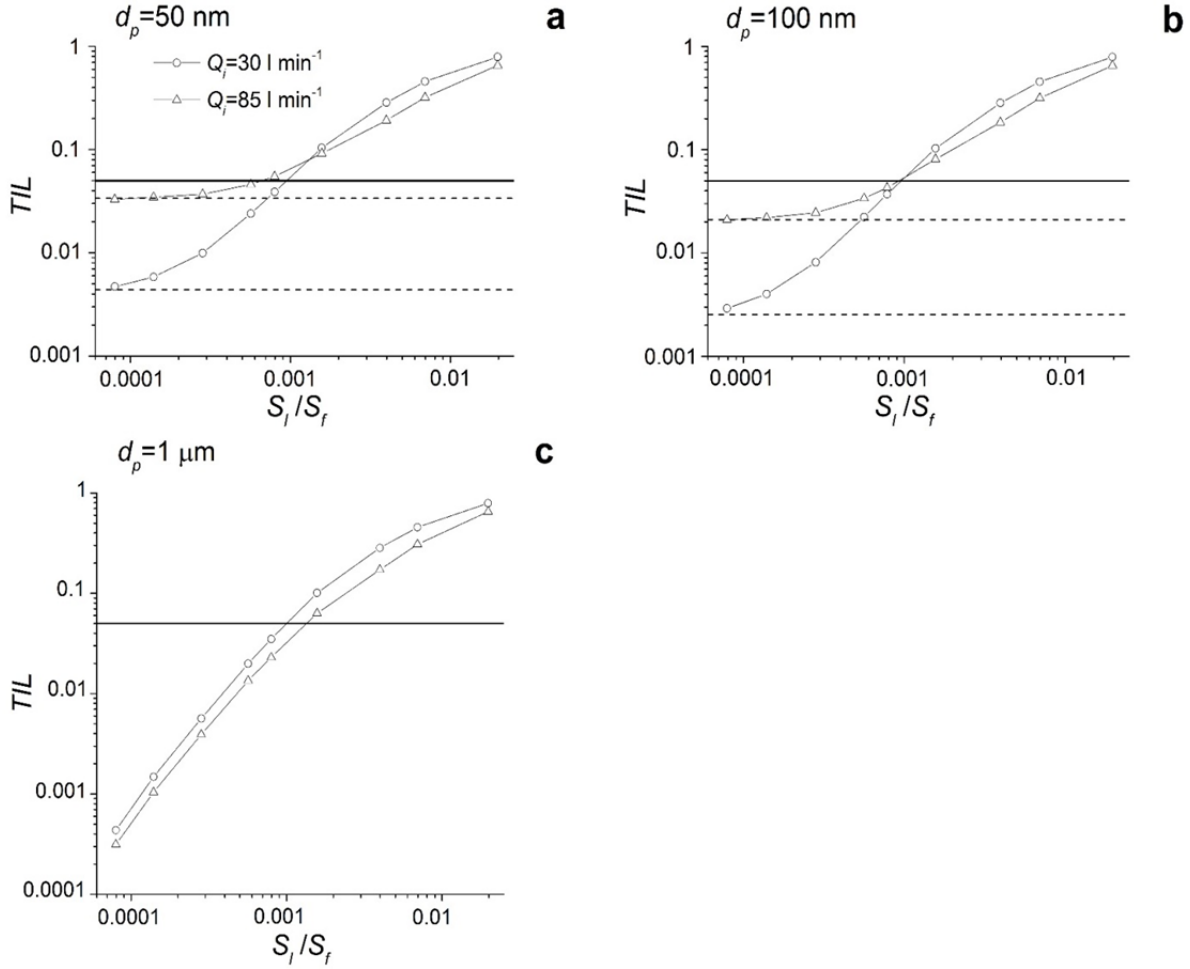

Fig. 6. *TIL* as a function of S_l/S_f calculated for Q_i = 30 and 85 L min^{-1} and d_p = 50 nm (a), 100 nm (b) and 1 μm (c). Solid lines represent the target value for an N95 (*TIL* = 0.05). Dotted lines represent a "perfect fit" respirator (with no faceseal leakage).

dimensions. The filter material permeability represented a conventional used N95 filter medium. The model demonstrated that the faceseal leakage substantially affects the protection offered by a facepiece. Once the leakage size reaches a certain threshold, the filter collection efficiency has essentially no influence on the respiratory protection, which now depends solely on the leakage size. The leakage-to-filter area ratio of ~10^{-3} can be considered as the threshold above which the faceseal leakage makes the N95 respirator unable to meet the 95% collection efficiency target (as

shown for inhalation flow rates of 30 and 85 L min^{-1} and the particle sizes from 50 nm to 1 μm). Under certain leakage condition (partially determined by the inhalation flow rate), the respirator protection level becomes independent on the particle size. The model developed in this effort can be deployed in future studies to investigate the performance of respirators with different filter permeability, facepiece geometry, etc. In addition, the model can be expanded to include the particle penetration dynamics due to the filter loading with the particles deposited on the fibers. This can be done by utilizing approaches presented in Kirsch (2006) and Dunnett and Clement (2009).

ACKNOWLEDGEMENT

This study was performed in the frameworks of the Russian Government Program of Competitive Growth at Kazan Federal University and supported by the Russian Foundation for Basic Research (grant No. 15-01-0613) and through a grant from the President of the Russian Federation (MK-6235.2015.1).

REFERENCES

ANSYS (2009) ANSYS FLUENT 12.0. User's Guide. Canonsburg: ANSYS Inc.

Anthony, T.R., and Flynn, M.R. (2005). Computational fluid dynamics investigation of particle inhalability. *J. Aerosol Sci.* 37: 750–765.

Anthony, T.R. (2010). Contribution of facial feature dimensions and velocity parameters on particle inhalability. *Ann. Occup. Hyg.* 54: 710–725.

Bałazy, A., Toivola, M., Reponen, T., Podgórski, A., Zimmer, A., and Grinshpun, S.A. (2006). Manikin-based performance evaluation of N95 filtering-facepiece respirators challenged with nanoparticles. *Ann. Occup. Hyg.* 50*:* 259–269.

Basu, A.J. and Khalili, A. (1999). Computation of flow through a fluid-sediment interface in a benthic chamber. *Phys. Fluids* 11: 1395–1405.

Bhattacharyya, S., Dhinakaran, S. and Khalili, A. (2006). Fluid motion around and through a porous cylinder. *Chem. Eng. Sci.* 61*:* 4451–4461.

Chen, C.C. and Willeke, K. (1992). Characteristics of face seal leakage in filtering facepieces. *Am. Ind. Hyg. Assoc. J.* 53: 533–539.

Cho, K.J., Reponen, T., Mckay, R., Shukla, R., Haruta, H., Sekar, P. and Grinshpun, S.A. (2010). Large particle penetration through N95 respirator filters and facepiece leaks with cyclic flow. *Ann. Occup. Hyg*. 54: 68–77.

Dunnett, S.J. and Vincent, J.H. (2000). A mathematical study of aerosol sampling by an idealised blunt sampler oriented at an angle to the wind: The role of gravity. *J. Aerosol Sci.* 31: 1187–1203.

Dunnett, S.J. and Clement, C.F. (2009). A numerical model of fibrous filters containing deposit. *Eng. Anal. Boundary Elem.* 33: 601–610.

Galeev, R.S. and Zaripov, S.K. (2003). A theoretical study of aerosol sampling by an idealized spherical sampler in calm air. *J. Aerosol Sci.* 34: 1135–1150.

Gougeon, R., Boulaud, D. and Renoux, A. (1996). Comparison of data from model fiber filters with diffusion, interception and inertial deposition models. *Chem. Eng. Commun*. 151: 19–39.

Gradon, L. and Yu, C.P. (1989). Diffusional particle deposition in the human nose and mouth. *Aerosol Sci. Technol.* 11: 231–220.

Grinshpun, S.A., Haruta, H., Eninger, R.M., Reponen, T., McKay, R.T. and Lee, S.A. (2009). Performance of an N95 filtering facepiece particulate respirator and a surgical mask during human breathing: Two pathways for particle penetration. *J. Occup. Environ. Hyg*. 6: 593–603.

He, X., Reponen, T., McKay, R. and Grinshpun, S.A. (2014). How does breathing frequency affect the performance of an N95 filtering facepiece respirator and a surgical mask against surrogates of viral particles? *J. Occup. Environ. Hyg.* 11: 178–185.

Hinds, W.C. (1998). *Aerosol Technology: Properties, Behavior, and Measurement of Airborne Particles*, John Wiley & Sons, Los Angeles, CA.

Hinds, W.C. and Kraske, G. (1987). Performance of dust respirators with facial seal leaks: I. Experimental. *Am. Ind. Hyg. Assoc. J*. 48: 836–841.

Kanaoka, C., Emi, H., Otani, Y. and Iiyama, T. (1987). Effect of charging state of particles on electret filtration. *Aerosol Sci. Technol.* 7: 1–13.

Kennedy, N.J. and Hinds, W. (2002). Inhalability of large solid particles. *J. Aerosol Sci.* 33: 237–255.

Kirsch V.A. (2006). Stokes flow past periodic rows of porous cylinders. *Theor. Found. Chem. Eng.* 40: 465–471.

Lee, S.A., Grinshpun, S.A., Adhikari, A., Li, W., Mckay, R., Maynard, A. and Reponen, T. (2005). Laboratory and field evaluation of a new personal sampling system for assessing the protection provided by the N95 filtering facepiece respirators against particles. *Ann. Occup. Hyg.* 49: 245–257.

Lei, Z., Yang, J., Zhuang, Z. and Roberge, R. (2013). Simulation and evaluation of respirator faceseal leaks using computational fluid dynamics and infrared imaging. *Ann. Occup. Hyg*. 57: 493–506.

Li, Y., Wong, T., Chung, J., Guo, Y.P., Hu, J.Y., Guan, Y.T., Yao, L., Song, Q.W. and Newton, E. (2006). In vivo protective performance of N95 respirator and surgical facemask. *Am. J. Ind. Med.* 49: 1056–1065.

Liu, B.Y.H., Lee, J.K., Mullins, H. and Danisch, S.G. (1993). Respirator leak detection by ultrafine aerosols: a predictive model and experimental study. *Aerosol Sci. Technol.* 19: 15–26.

Myers, W.R., Allender, J., Plummer, R. and Stobbe, T. (1986). Parameters that bias the measurement of airborne concentration within a respirator. *Am. Ind. Hyg. Assoc. J*. 47: 106–114.

NIOSH (1996). National Institute for Occupational Safety and Health: NIOSH Guide to the Selection and Use of Particulate respirators Certified under 42 CFR 84, DHHS (NIOSH) Pub. No. 96-101. NIOSH, Cincinnati, OH.

Nield, D.A. and Bejan, A. (1992). *Convection in Porous*

Media, Springer, New York.

Payet, S., Boulaud, D., Madelaine, G. and Renoux, A. (1992). Penetration and pressure drop of a HEPA filter during loading with submicron liquid particles. *J. Aerosol Sci*. 23: 723–735.

Pich, J. (1966). Theory of Aerosol Filtration by Fibrous and Membrane Filters. In *Aerosol Science Book*, Davies, C.N. (Ed.), pp. 223–286.

Rengasamy, S., and Eimer, B.C. (2011). Total inward leakage of nanoparticles through filtering facepiece respirators. *Ann. Occup. Hyg*. 55: 253–263.

Rengasamy, S., and Eimer, B.C. (2012). Nanoparticle penetration through filter media and leakage through face seal interface of N95 filtering facepiece respirators. *Ann. Occup. Hyg*. 56: 568–580.

Roberge, R.J., Bayer, E., Powell, J.B., Coca, A., Roberge, M.R. and Benson, S.M. (2010). Effect of exhaled moisture on breathing resistance of N95 filtering facepiece respirators. *Ann. Occup. Hyg.* 54: 671–677.

Yang, J., Dai, J. and Zhuang, Z. (2009). Simulating the interaction between a respirator and a headform using LS-DYNA. *Comput.-Aided Des. Applic.* 6: 539–551.

Zaripov, S.K., Gilfanov, A.K. and Mukhametzanov, I.T. (2014). Performance of spherical aerosol sampler in low–velocity agriculture environment. *Acta Hort. (ISHS)* 1054: 333–339.

Zhang, Y. (2004). *Indoor Air Quality Engineering*, Taylor and Francis (CRC Press), Boca Raton, FL, 255.

Received for review, August 10, 2015
Revised, February 28, 2016
Accepted, March 1, 2016